3.1 Introduction

Forming a carbon-carbon unsaturated bond by oxidative coupling reaction has been of prime importance in organic synthesis. Oxidative coupling has rapidly developed over the past two decades as it has great potential for green, economical, and environment-friendly synthesis [1, 2]. Molecules with unsaturated bonds are widely found in natural compounds [3] and commonly used in pharmaceuticals, agrochemicals, functional materials, etc [4, 5]. Indole derivatives containing carbon-carbon unsaturated bonds have shown extensive biological activities like anti-HIV [6], antiviral [7], anticonvulsants [8], and antitumor agents [9].

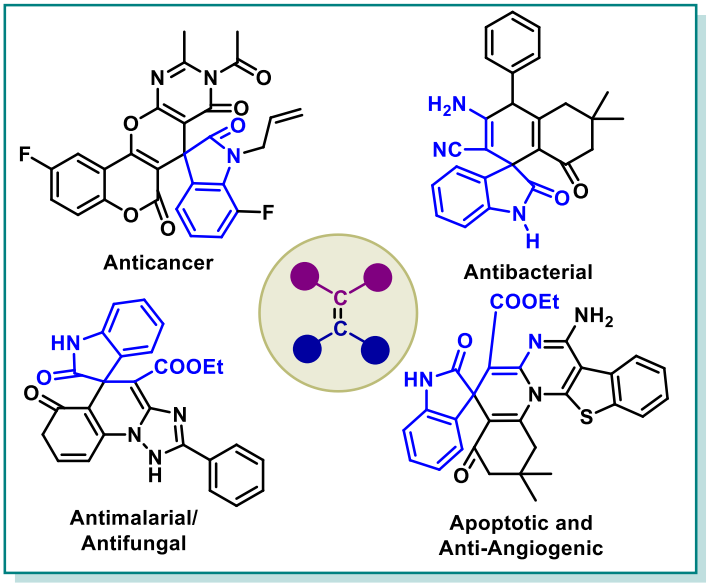

Figure 3.1 Biologically active oxindole compounds

3-Alkylidene oxindoles are essential intermediates in synthesizing various heterocyclic compounds [10-12]. Such compounds are potential drugs, such as chiral spirooxindole-pyranopyrimidines with anticancer activity [13], spiro[indole-3,40-quinolines] with antibacterial activity [14], and derivatives of cyclic spiro-2-oxindoles with antimicrobial

activity [15]. These compounds also act as apoptotic and Anti-angiogenic agents [16] (Figure 3.1).

In recent years, chemists have emphasized the use of visible light in green organic synthesis as it is a natural, unmingled, economical, easily practicable, renewable, and environmentally promising energy source [17-21]. These reactions also have superiority over metal-catalyzed reactions as metal-catalyzed reactions have harsh reaction conditions, poor yields, complex workup, and the use of environmentally harmful and costly chemicals [22-24]. Many organic reactions are accelerated by photoredox catalysts using eosin Y as a facile and convincing tool for activating organic molecules in visible-light-driven organic synthesis [25-27]. Eosin Y is a metal-free organic dye used as a tempting alternative to transition metal complexes as they are relatively cheaper and less toxic [28-30].

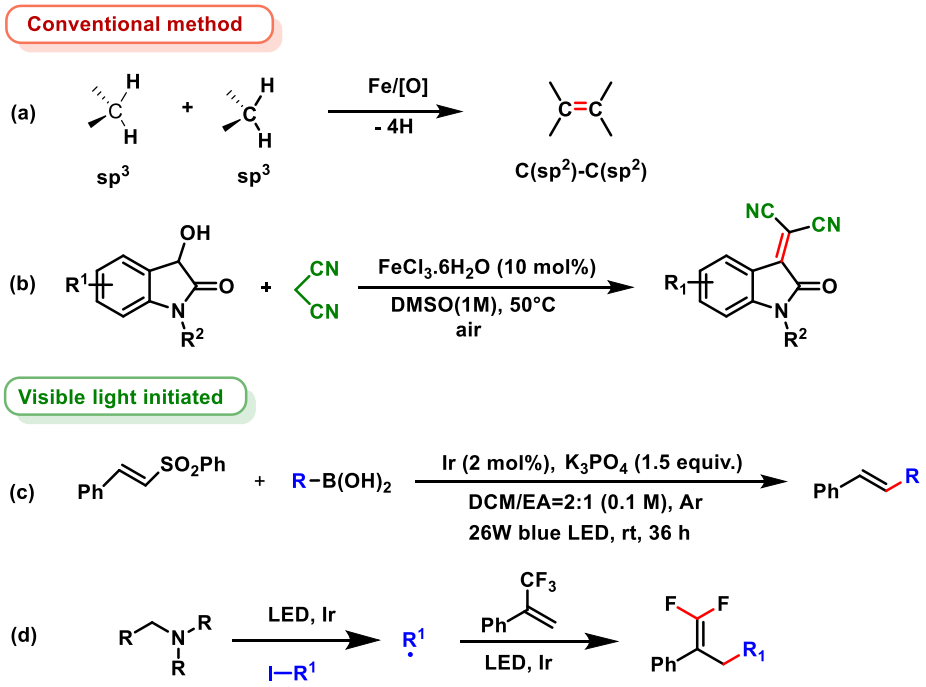

Scheme 3.1 Previous methods for synthesis of carbon-carbon double bonds

Few methodologies i.e., conventional [31, 32] and visible-light-initiated [33, 34] approaches have been previously reported to synthesize carbon-carbon double bonds (Scheme 3.1). They also suffer some drawbacks like complex workup, low yield, large waste generation, and are environmentally unfriendly. Also, as far as we know, there is no report on the direct oxidative coupling of indole and active methylene compounds. Hence, there is a great need to develop inexpensive and environment-friendly methods instead of metal catalysts that adversely impact the environment.

Because of those mentioned above and the ongoing interest in developing green, environmentally benign, and sustainable methods, we have reported a new method for the oxidative coupling of indole and active methylene compounds using eosin Y as a photocatalyst under visible light conditions using atmospheric air and as an oxidant which is readily available, and environmentally friendly (Scheme 3.2).

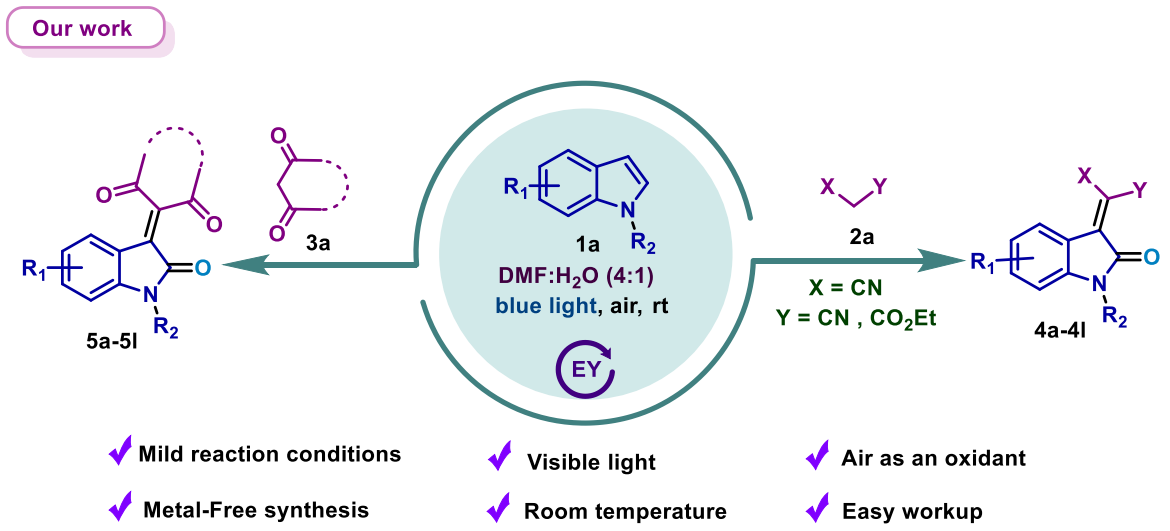

Scheme 3.2 Our work on oxidative coupling of indole and active methylene compounds

3.2 Results and Discussion

We first thought of developing a new methodology for the oxidative coupling of indole and active methylene molecules. We have taken a model reaction, indole (1mmol) and malononitrile (1mmol), using various solvents and different photocatalysts under visible-light-irradiation. Initially, we tested the role of various photocatalysts like rose bengal, rhodamine B, xanthone, and eosin Y (Table 3.1, entries 1-4) for the reaction using DMF as solvent. Unfortunately, we obtained a small amount of product **4a** for the first three photocatalysts and a 15% yield with eosin Y as a photocatalyst. Further, we optimized our reaction using different solvents like DMSO, ethanol, acetonitrile, and DCE (Table 3.1, entries 5-8). But none of them could provide the expected yield of the product. Encouraged by the result, we optimized our reaction with the different molar proportions of DMF:Water like (1:1, 1:2, 2:1, 3:1, 3:2, and 4:1) (Table 3.1, entries 9-14). However, we were appalled to observe excellent yield when the molar proportion was 4:1 (Table 3.1, entry 14). We also inspected the effect of time variation on product yield and found that yield decreases by decreasing the reaction time (Table 3.1, entries 15-17).

To find the optimal intensity of visible light, the model reaction was performed under visible light sources of different intensities (8 W, 12 W, 18 W, 22 W, and 32 W) and green and white LED (Table 3.2). The best result was obtained with a 22 W blue LED. After that, the yield became constant on increasing the intensity (Figure 3.2).

Table 3.1 Optimization table for reaction conditions [(a)]

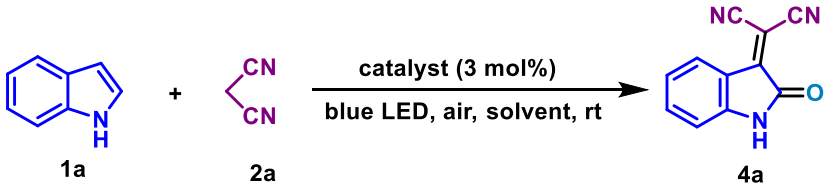

Entry	Catalyst	Solvent	Water Content	Time (h)	Yield [(b)] (%)
1	Rose bengal	DMF	0	24	6
2	Rhodamine B	DMF	0	24	trace
3	xanthone	DMF	0	24	3
4	Eosin Y	DMF	0	24	15
5	Eosin Y	DMSO	0	24	trace
6	Eosin Y	C_2H_5OH	0	24	NA[c]
7	Eosin Y	CH_3CN	0	24	NA
8	Eosin Y	DCE	0	24	NA
9	Eosin Y	DMF: H_2O	1:1	24	41
10	Eosin Y	DMF: H_2O	1:2	24	37
11	Eosin Y	DMF: H_2O	2:1	24	46
12	Eosin Y	DMF: H_2O	3:1	24	62
13	Eosin Y	DMF: H_2O	3:2	24	51
14	Eosin Y	DMF: H_2O	4:1	24	88
15	Eosin Y	DMF: H_2O	4:1	22	82
16	Eosin Y	DMF: H_2O	4:1	20	79
17	Eosin Y	DMF: H_2O	4:1	18	74

[(a)]Reaction Condition : indole (1 mmol), malanonitrile (1 mmol), catalyst (3 mol%), reaction volume (5 mL), 22 W Blue LED (24 h) under open air at room temperature. [(b)]isolated yield [(c)]no Reaction

Table 3.2 Optimization of LED intensities [a]

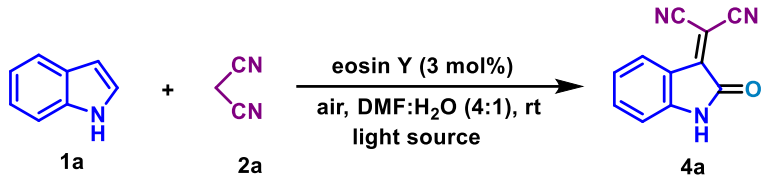

Entry	LED (W)	Time (h)	Yield [b] (%)
1	8	24	60
2	12	24	67
3	18	24	76
4	22	24	88
5	32	24	88
6	green	24	77
7	white	24	71

[a]Reaction Condition: indole (1 mmol), malononitrile (1 mmol), eosin Y (3 mol%), reaction volume (5 mL), different blue LEDs (24 h) under open air at room temperature [b]isolated yield

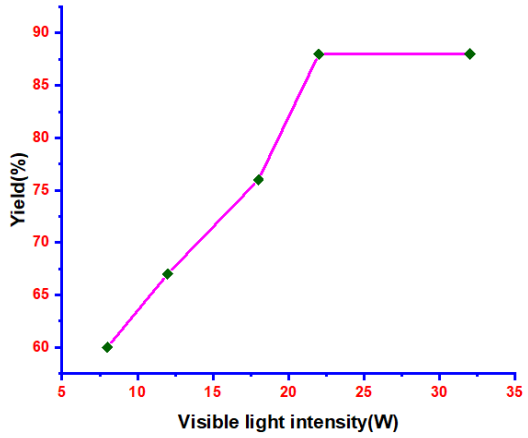

Figure 3.2 Yield (%) vs Visible light intensity (W) for the preparation of 2-(2-oxoindolin-3-ylidene) malononitrile

Table 3.3 Substrate scope of aliphatic compounds [(a)]

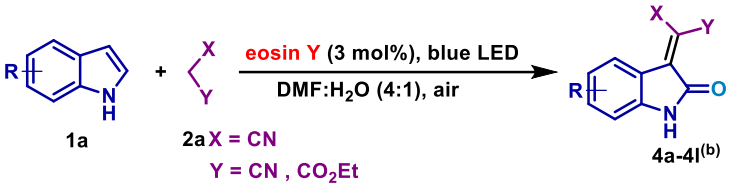

scope of indoles with acyclic active methylene compounds

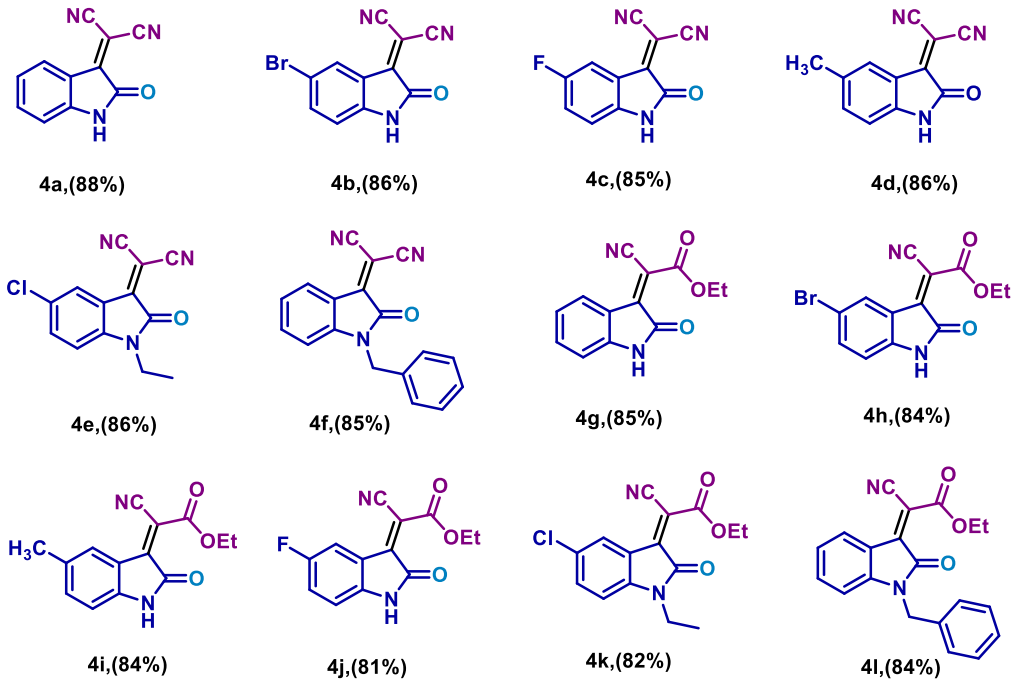

[(a)]Reaction Condition: **1a** (1 mmol), **2a** (1 mmol), eosin Y (3 mol%), reaction volume (5 mL), 22 W Blue LED (24 h) under open air at room temperature, [(b)]isolated yield

After establishing the optimal conditions, we then started analyzing the adaptability with different substituted indoles to explore the scope of the oxidative coupling reaction. We were pleased by the diversity of this methodology. As revealed in tables 2.3 and 3.4, the indole having electron-donating or electron-withdrawing groups reacted smoothly with different active methylene molecules to deliver the desired products in good to excellent yields (**4a-4l, 5a-5m**). Various functional groups including chloro, bromo, fluoro, and methyl were well

tolerated in the 5th position of indole, giving the respective products a high yield. Furthermore, Table 3.3 shows that various substituted indole reacted with malononitrile, giving high yields (88%) of products (**4a-4f**) and relatively lower results (85%) with ethyl cyanoacetate (**4g-4l**).

Table 3.4 Substrate scope of aromatic compounds [a]

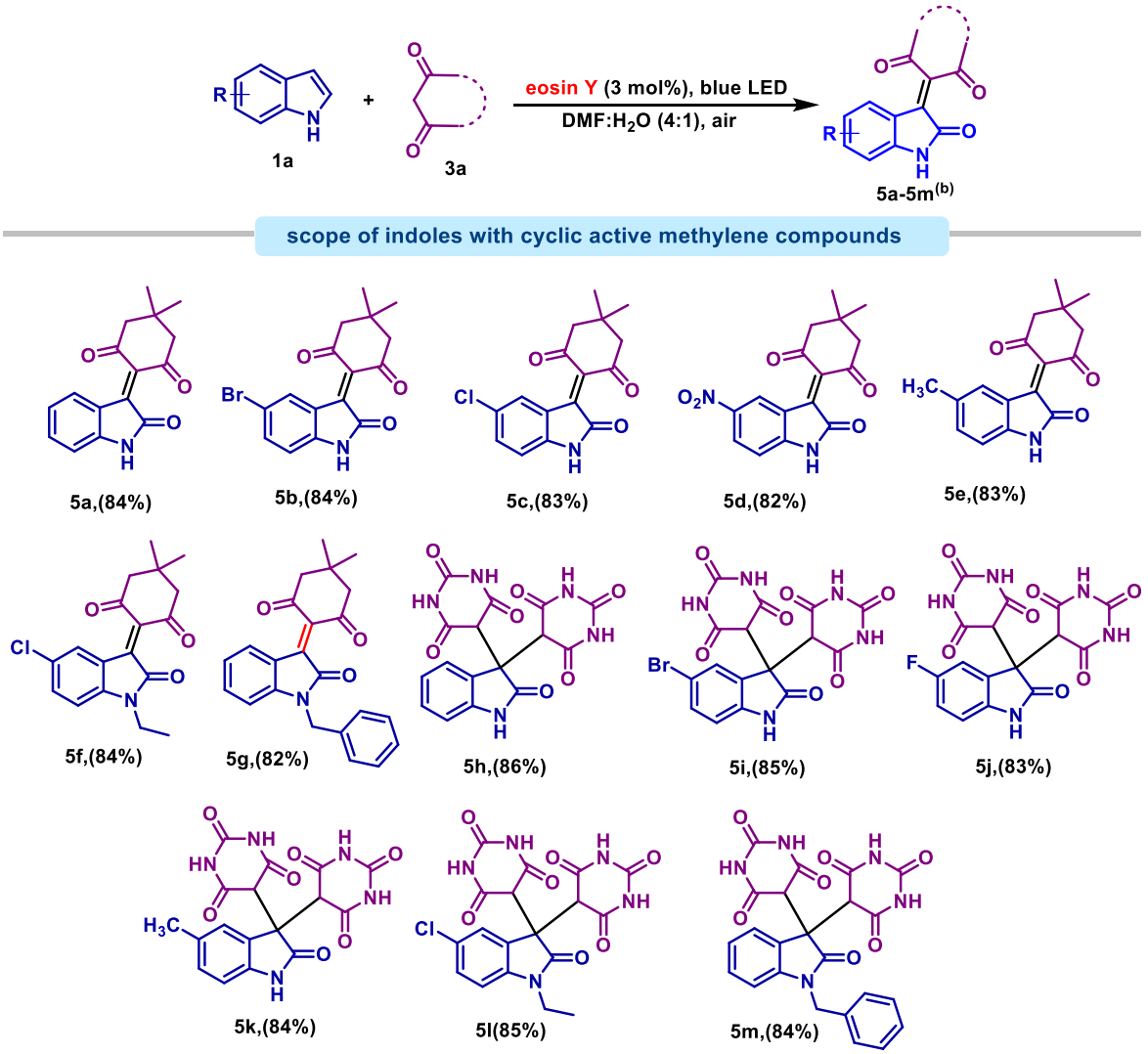

[a]Reaction Condition: **1a** (1mmol), **3a** (1mmol), eosin Y (3 mol%), reaction volume (5 mL), 22 W Blue LED (24 h) under open air at room temperature, [b]isolated yield

To expand the utility of our methodology, we then tried to employ cyclic active methylene compounds, dimedone and barbituric acid in the reaction (Table 3.4). Different indole derivatives yielded good to excellent amount of desired products. Interestingly, two molecules of barbituric acid reacted with indole (**5h-5m**), whereas only one molecule of dimedone reacted with indole (**5a-5g**).

To find the reactivity pattern of indole with malononitrile, ethyl cyanoacetate, dimedone, and barbituric acid and also to confirm the above observation, the effect of the molar proportion of the reactant on the reaction was examined (Table 3.5). The study of this table indicates that the best outcomes were achieved using indole, malononitrile; indole, ethyl cyanoacetate; indole, dimedone; in the molar proportion 1.0: 1.0 (Table 3.5, entry 1, 6, 11), and indole, barbituric acid in the molar proportion 1.0: 2.0 (Table 3.5, entry 17) using DMF:water (4:1) as a solvent with 22 W blue LED. The perusal of this table also indicates that there is only a change in the yield of the product and no change in the type of the product on changing the molar proportion of the reactants.

Table 3.5 Effect of molar ratio of the substrate on the yield of products 4 and 5 [(a)]

Entry No.	Substrate	Molar ratio of substrate	% Yields[(b)]	Product
1.	Indole : Malononitrile	1:1	88	4a
2.	Indole : Malononitrile	1:2	80	4a
3.	Indole : Malononitrile	2:1	40	4a
4.	Indole : Malononitrile	1:3	72	4a
5.	Indole : Malononitrile	1:4	54	4a
6.	Indole: Ethyl cyanoacetate	1:1	85	4g

7.	Indole : Ethyl cyanoacetate	1:2	80	4g
8.	Indole: Ethyl cyanoacetate	2:1	39	4g
9.	Indole: Ethyl cyanoacetate	1:3	70	4g
10.	Indole: Ethyl cyanoacetate	1:4	49	4g
11.	Indole : Dimedone	1:1	84	5a
12.	Indole : Dimedone	1:2	42	5a
13.	Indole : Dimedone	2:1	76	5a
14.	Indole : Dimedone	1:3	66	5a
15.	Indole : Dimedone	1:4	47	5a
16.	Indole : Barbituric acid	1:1	39	5h
17.	Indole : Barbituric acid	1:2	86	5h
18.	Indole : Barbituric acid	2:1	41	5h
19.	Indole : Barbituric acid	1:3	69	5h
20.	Indole : Barbituric acid	1:4	41	5h

[(a)]Reaction Condition: substrates, eosin Y (3 mol%), reaction volume (5 mL), 22 W Blue LED (24 h) under open air at room temperature, [(b)]isolated yield

3.3 Control Experiment

We shifted our experimentation towards mechanistic pathways with optimized standard reaction conditions and broad substrate scope and performed a few control experiments. In the beginning, we performed a reaction of indole (**1a**) and malononitrile (**2a**) under N_2 atmosphere and anhydrous conditions. We got a trace amount of **4a** (Scheme 3.3, reaction A), which implies the importance of oxygen and water in the reaction. We also saw no reaction in the dark (Scheme 3.3, reaction D), which confirms the importance of light for this

reaction. Further, with the addition of TEMPO (2,2,6,6-tetramethyl-1-piperidinyloxy) (3 equivalent), BHT (3 equivalent), and benzoquinone, a radical scavenger, the amount of **4a** was sharply decreased (Scheme 3.3, reaction B, C, E respectively).

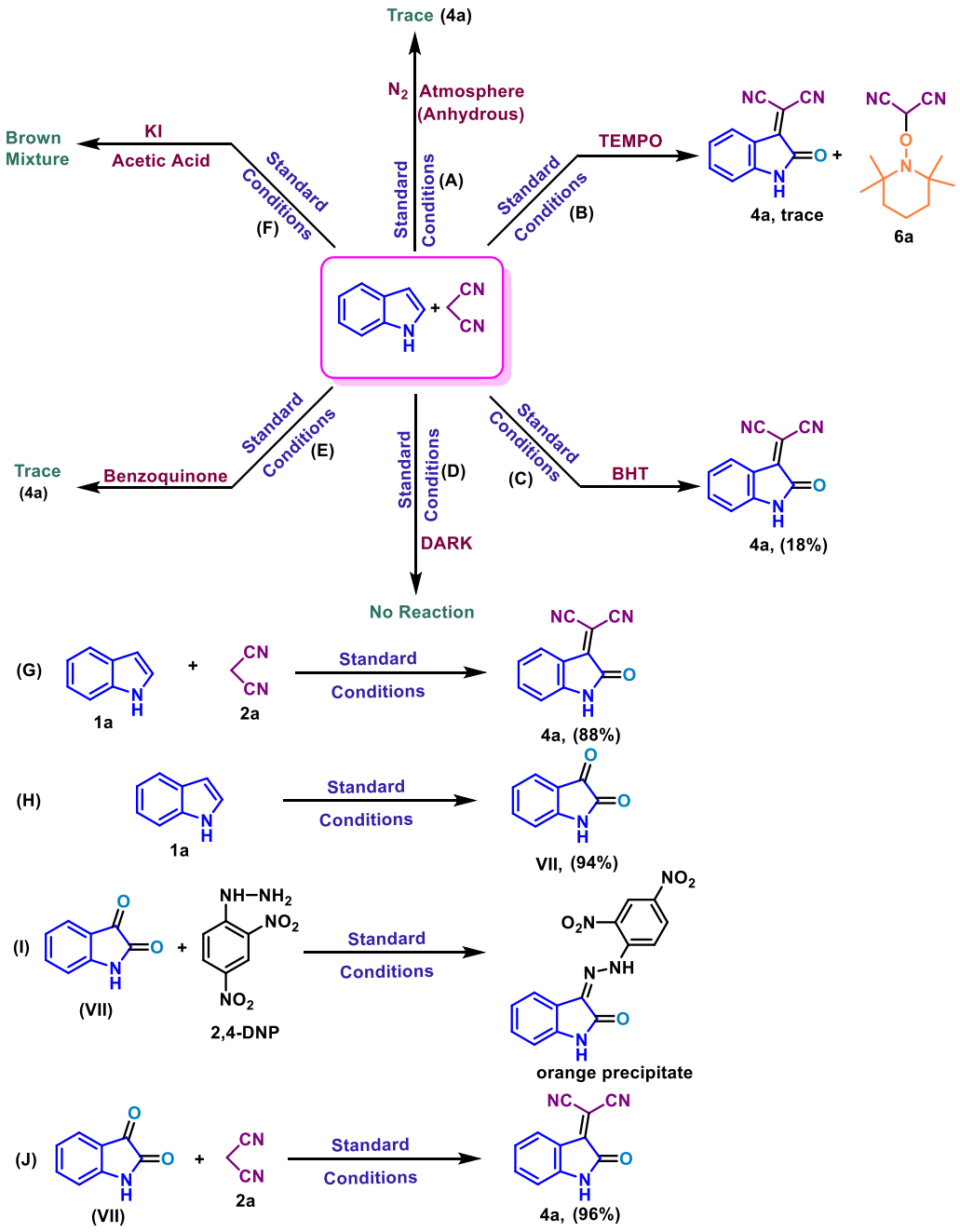

Scheme 3.3 Mechanistic Investigation

The free radical mechanism was further confirmed by the adduct (**6a**) formation which was characterized by ^{1}H and ^{13}C NMR spectroscopy. Additionally, we investigated the formation of H_2O_2 by adding the reaction mixture to the freshly prepared solution of KI and acetic acid [35] (Scheme 3.3, reaction F). The reaction mixture turned brown due to the liberation of iodine. The formation of H_2O_2 indicates the formation of superoxide radical anion species.

In order to find the path of the reaction, some more control experiments were carried out. When the reaction of indole (**1a**) and malononitrile (**2a**) was performed under standard conditions, product **4a** was obtained with an 88% yield (Scheme 3.3, reaction G). To identify the intermediate, the reaction of indole was carried out under standard conditions alone, and intermediate, i.e., isatin (**VII**), was formed (Scheme 3.3, reaction H). The intermediate (**VII**) formation was confirmed through its characterization by ^{1}H and ^{13}C NMR spectroscopy. Also, to establish the intermediacy of isatin (**VII**), the isatin reaction was carried out under standard conditions in the presence of 2,4-DNP, and the orange precipitate was formed (Scheme 3.3, reaction I). However, the reaction of isatin (**VII**) and malononitrile **2a** was performed under a similar condition. The formation of product **4a** in 96% yield also confirms the intermediacy of isatin (**VII**) (Scheme 3.3, reaction J). We conducted an "ON-OFF" experiment (Figure 3.3) to analyze the effect of visible light on the reaction. This experiment showed that visible light could significantly boost the reaction.

3.3.1 ON-OFF Experiments

Under the set reaction conditions, a reaction between **1a** and **2a** was carried out on a scale of 1 mmol. Successive periods of stirring the reaction mixture in the presence of visible light

(blue LED) and then stirring in the absence of light were conducted. Each time, a time point was reached, one reaction system was suspended, and it was later purified using column chromatography to yield the appropriate product **4a**.

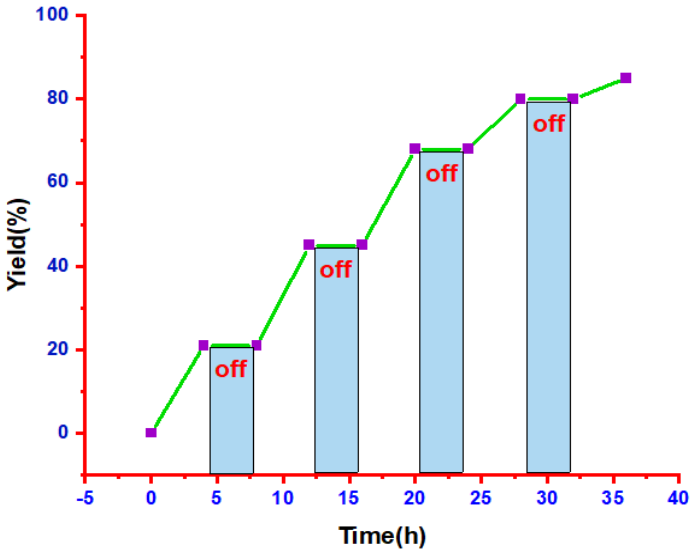

Figure 3.3 ON-OFF experiment

3.4 Proposed Mechanism

The following plausible mechanism was proposed based on the preceding reports [36, 37] and control experiments (Scheme 3.4). Upon exposure to visible light, excited eosin Y (EY*) was formed from eosin Y (EY). Oxygen quenched the excited eosin Y (EY*) to form singlet oxygen which reacts with indole (**1a**) and leads to the formation of peroxo species (**II**). The second photocatalytic cycle oxidized species (**II**) to form peroxoindole species (**III**) and formed radical anion $EY^{\cdot -}$. The cation (**IV**) and hydroxyl radical were sequentially formed by the cleavage of species (**III**). Formed hydroxyl radical abstracts hydrogen atom from (**IV**) and provides (**V**).

The reported value for the $E^0_{(red)}$ of the excited state of eosin Y is -1.32 V vs SCE, which is sufficient for the reduction of oxygen to its superoxide radical anion ($E^0_{(red)}$ is -0.56 V vs SCE). Hence $EY^{\cdot-}$ reduced oxygen to form superoxide radical anion.

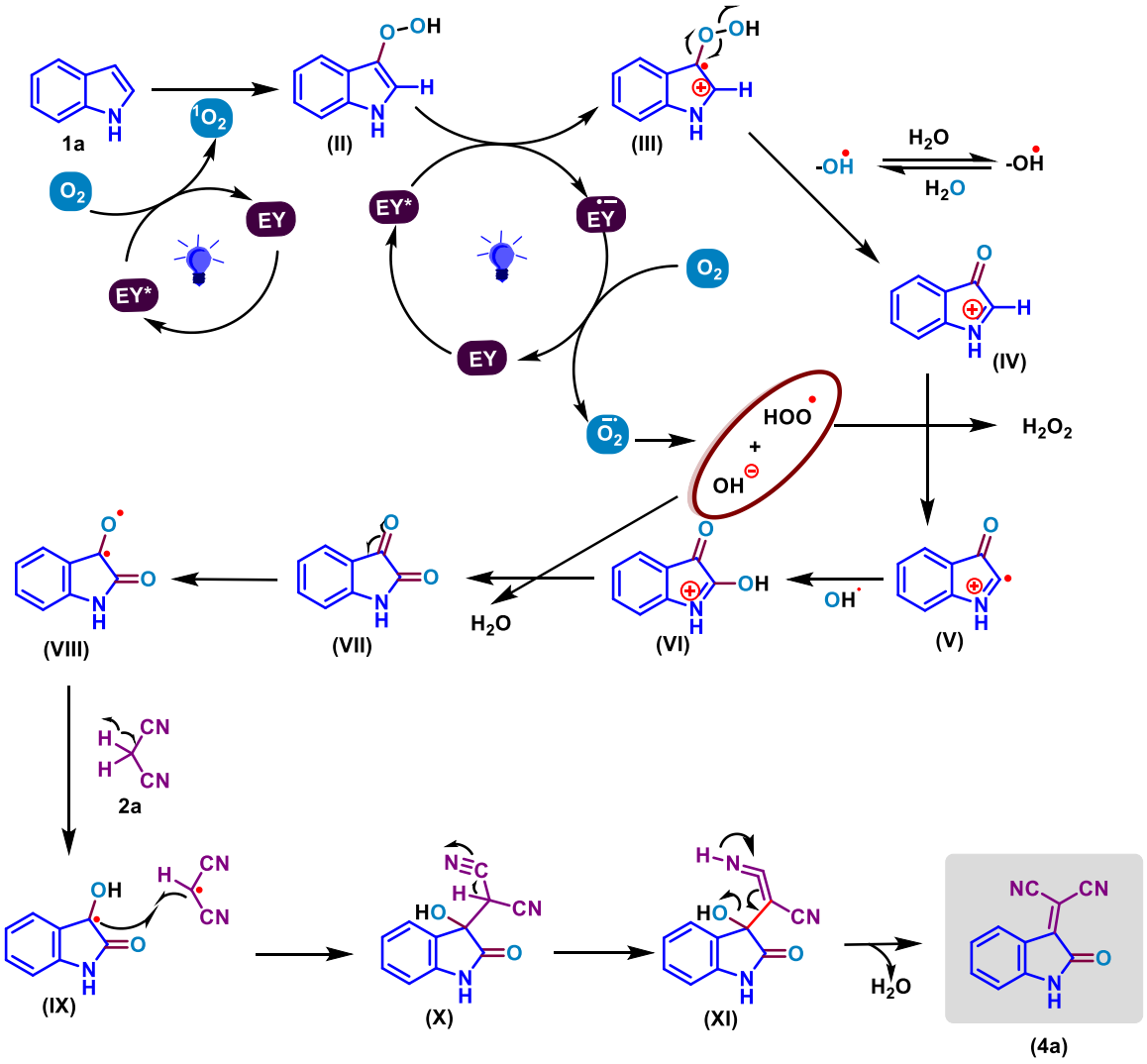

Scheme 3.4 Plausible mechanism

The radical anion forms hydroxide anions and peroxide radicals upon reaction with water. The intermediate (**VII**) was formed from species (**VI**) (by the release of a water molecule)

which was in turn formed by the reaction of radical species (**V**) and hydroxyl radical. The free radical of intermediate (**VII**) was formed by irradiating visible light, which abstracts hydrogen radical from malononitrile (**2a**) and leads to the formation of the desired product (**4a**) by removing water.

3.5 Conclusion

In summary, a novel and efficient visible-light-mediated oxidative coupling of indole and active methylene compounds has been developed using eosin Y as a green and sustainable photocatalyst. The reaction occurs efficiently under milder conditions and virtually in assessable yield of the desired coupling products. This approach displays outstanding functional group compatibility with both electron-donating and electron-withdrawing indole. It is also associated with some additional features like metal-free reaction, high yield of the products, no side product, and use of renewable energy sources.

3.6 Experimental Procedures

3.6.1 General procedure for synthesis of compounds 4a- 4l and 5a-5m

Indole (1 mmol), eosin Y (3mol %), and DMF:H_2O (4:1) were taken in a 10 mL RB flask. The resulting mixture was stirred in the open air for 8 h under visible-light-irradiation. After that, malononitrile or active methylene compounds (1 mmol) were added to the reaction mixture. The progress of the reaction was monitored via TLC. The precipitate obtained was filtered and washed with ethanol after the completion of the reaction. The desired product was obtained in good yields after recrystallization using ethanol.

3.7 Characterization of products

2-(2-Oxoindolin-3-ylidene) malononitrile (4a)

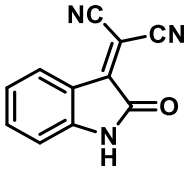

88% yield; brick red crystal; m.p. 196°C; **^{1}H NMR** (500 MHz, DMSO-d_6) δ 11.22 (s, 1H), 7.87 (d, *J* = 7.6 Hz, 1H), 7.57 (m, 1H), 7.13 (t, *J* = 7.7 Hz, 1H), 6.93 (d, *J* = 7.9 Hz, 1H). **^{13}C NMR** (126 MHz, DMSO-d_6) δ 164.21, 151.08, 146.93, 138.28, 126.28, 123.38, 119.09, 113.52, 112.10, 81.06. **HRMS** (ESI) m/z: $[M + H]^+$ calculated for $C_{11}H_6N_3O$: 196.0510; found: 196.0509.

2-(5-Bromo-2-oxoindolin-3-ylidene) malononitrile (4b)

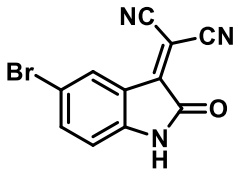

86% yield; purple crystal; m.p. 225°C; **^{1}H NMR** (500 MHz, DMSO-d_6) δ 11.37 (s, 1H), 7.92 (d, *J* = 7.7 Hz, 1H), 7.76 (m, 1H), 6.94 (d, *J* = 7.4 Hz, 1H). **^{13}C NMR** (126 MHz, DMSO-d_6) δ 177.85, 163.94, 163.78, 149.98, 145.99, 140.10, 128.10, 120.99, 114.37, 114.13. **HRMS** (ESI) m/z: $[M + H]^+$ calculated for $C_{11}H_5BrN_3O$: 273.9615; found: 273.9613.

2-(5-Fluoro-2-oxoindolin-3-ylidene) malononitrile (4c)

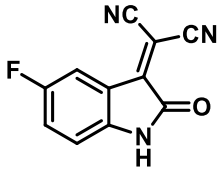

85% yield; purple crystal; m.p. 245°C; **^{1}H NMR** (500 MHz, DMSO-d_6) δ 11.95 (s, 1H), 8.63 (d, *J* = 7.6 Hz, 1H), 8.44 (m, 1H), 7.13 (s, 1H). **^{13}C NMR** (126 MHz, DMSO-d_6) δ 164.44, 151.62, 149.70, 142.82, 133.12, 121.11, 119.20, 112.36, 83.88. **HRMS** (ESI) m/z: $[M + H]^+$ calculated for $C_{11}H_5FN_3O$: 214.0416; found: 214.0412 . **^{19}F NMR** (471 MHz, DMSO-d6) δ -120.02, -120.06.

2-(5-Methyl-2-oxoindolin-3-ylidene) malononitrile (4d)

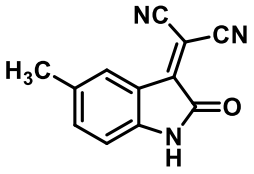

86% yield; reddish crystal; m.p. 183°C; **^{1}H NMR** (500 MHz, DMSO-d_6) δ 11.11 (s, 1H), 7.65 (s, 1H), 7.40 (m, 1H), 6.84 (d, *J* = 8.0 Hz, 1H), 2.28 (s, 3H). **^{13}C NMR** (126 MHz, DMSO-d_6) δ 164.27, 151.05, 144.89, 139.01, 132.39, 126.17, 119.12, 113.54, 111.98, 80.74, 20.92. **HRMS** (ESI) m/z: $[M + H]^+$ calculated for $C_{12}H_8N_3O$: 210.0667; found: 210.0665.

2-(5-Chloro-1-ethyl-2-oxoindolin-3-ylidene) malononitrile (4e)

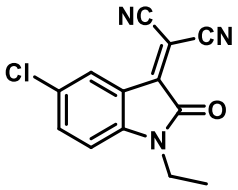

86% yield; black crystal; m.p. 190°C; **^{1}H NMR** (500 MHz, $CDCl_3$) δ 8.11 (d, *J* = 7.7 Hz, 1H), 7.56 (m, 1H), 6.86 (d, *J* = 7.5 Hz, 1H), 3.79 (t, 2H), 1.31 (t, 3H). **^{13}C NMR** (126 MHz, $CDCl_3$) δ 161.72, 148.41, 144.65, 137.18, 129.35, 126.60, 119.33, 111.86, 110.72, 110.21, 84.08, 35.43, 12.42. **HRMS** (ESI) m/z: $[M + H]^+$ calculated for $C_{13}H_9ClN_3O$: 258.0434; found: 258.0428.

2-(1-Benzyl-2-oxoindolin-3-ylidene) malononitrile (4f)

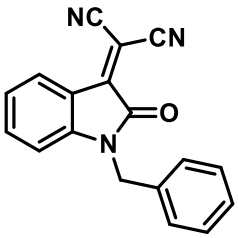

85% yield; purple solid;, m.p. 201°C; **^{1}H NMR** (500 MHz, $CDCl_3$) δ 8.16 (m, 1H), 7.52 – 7.45 (m, 1H), 7.37 – 7.28 (m, 5H), 7.18 – 7.09 (m, 1H), 6.80 (m, 1H), 4.94 (d, 2H). **^{13}C NMR** (126 MHz, $CDCl_3$) δ 137.70, 129.12, 128.51, 128.35, 127.53, 127.01, 123.97, 88.65, 88.49, 44.22. **HRMS** (ESI) m/z: $[M + H]^+$ calculated for $C_{18}H_{12}N_3O$: 286.0980; found: 286.0979.

Ethyl-2-cyano-2-(2-oxoindolin-3-ylidene) acetate (4g)

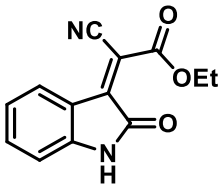

85% yield; dark red crystal; m.p. 220°C; **^{1}H NMR** (500 MHz, DMSO-d_6) δ 11.10 (s, 1H), 8.10 (d, *J* = 7.7 Hz, 1H), 7.49 – 7.42 (m, 1H), 7.01 (d, *J* = 0.7 Hz, 1H), 6.87 (d, *J* = 7.6 Hz, 1H), 4.39 (m, 2H), 1.27 (m, 3H). **^{13}C NMR** (126 MHz, DMSO-d_6) δ 165.66, 161.81, 146.28, 145.79, 138.85, 136.53, 129.70, 122.65, 119.16, 111.33, 104.94, 63.61, 14.23. **HRMS** (ESI) m/z: $[M + H]^+$ calculated for $C_{13}H_{11}N_2O_3$: 243.0769; found: 243.0769.

Ethyl-2-(5-bromo-2-oxoindolin-3-ylidene)-2-cyanoacetate (4h)

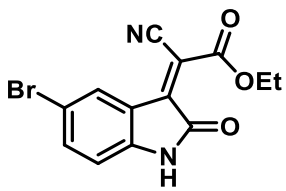

84% yield; white crystal; m.p. 226°C; **^{1}H NMR** (500 MHz, DMSO-d_6) δ 11.20 (s, 1H), 8.19 (s, 1H), 7.52 (s, 1H), 6.88 (d, *J* = 7.7 Hz, 1H), 4.46 – 4.32 (m, 2H), 1.39 – 1.23 (m, 3H). **^{13}C NMR** (126 MHz, DMSO-d_6) δ 165.45, 161.62, 145.21, 135.67, 129.41, 114.27, 112.55, 13.98. **HRMS** (ESI) m/z: $[M + H]^+$ calculated for $C_{13}H_{10}BrN_2O_3$: 320.9874; found: 320.9871.

Ethyl-2-cyano-2-(5-methyl-2-oxoindolin-3-ylidene) acetate (4i)

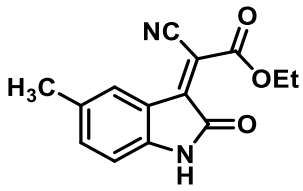

84% yield; red crystal; m.p. 220°C; **^{1}H NMR** (500 MHz, DMSO-d_6) δ 10.99 (s, 1H), 7.93 (s, 1H), 7.30 (d, *J* = 8.0 Hz, 1H), 6.79 (d, *J* = 8.0 Hz, 1H), 4.45 (m, 2H), 2.26 (d, *J* = 6.5 Hz, 3H), 1.35 (t, *J* = 7.1 Hz, 3H). **^{13}C NMR** (126 MHz, DMSO-d_6) δ 165.76, 161.87, 145.90, 144.08, 137.14, 131.53, 129.82, 119.19, 114.71, 111.15, 63.65, 21.06, 14.22. **HRMS** (ESI) m/z: $[M + H]^+$ calculated for $C_{14}H_{13}N_2O_3$: 257.0926; found: 257.0922.

Ethyl-2-cyano-2-(5-fluoro-2-oxoindolin-3-ylidene) acetate (4j)

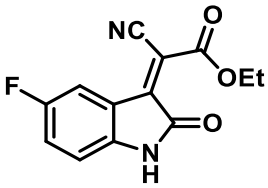

81% yield; brown crystal; m.p. 228°C; **^{1}H NMR** (500 MHz, DMSO-d_6) δ 11.13 (d, *J* = 7.1 Hz, 1H), 8.02 (d, *J* = 6.4 Hz, 1H), 7.44 – 7.32 (m, 1H), 6.96 – 6.84 (m, 1H), 4.50 – 4.37 (m, 2H), 1.35 (m, *J* = 7.1 Hz, 3H). **^{13}C NMR** (126 MHz, DMSO-d_6) δ 173.38, 165.55, 156.59, 139.10, 137.47, 124.36, 116.34, 115.46, 111.05, 109.77, 103.06, 59.65, 16.55. **^{19}F NMR** (471 MHz, DMSO-d_6) δ -120.44, -121.19. **HRMS** (ESI) m/z: $[M + H]^+$ calculated for $C_{13}H_{10}FN_2O_3$: 261.0675; found: 261.0671.

Ethyl-2-(5-chloro-1-ethyl-2-oxoindolin-3-ylidene)-2-cyanoacetate (4k)

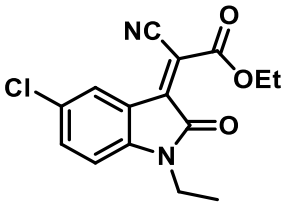

82% yield; black crystal; m.p. 213°C; **^{1}H NMR** (500 MHz, $CDCl_3$) δ 8.40 (s, 1H), 7.47 – 7.44 (m, 1H), 6.79 (d, *J* = 7.6 Hz, 1H), 4.51 – 4.48 (m, 2H), 3.81 (d, 2H), 1.47 (t, 3H), 1.29 (d, 3H). **^{13}C NMR** (126 MHz, $CDCl_3$) δ 163.56, 161.26, 144.19, 135.13, 134.14, 130.12, 128.40, 125.34, 120.00, 110.08, 109.72, 63.71, 35.21, 13.97, 12.38. **HRMS** (ESI) m/z: $[M + H]^+$ calculated for $C_{15}H_{14}ClN_2O_3$: 305.0692; found: 305.0690.

Ethyl-2-(1-benzyl-2-oxoindolin-3-ylidene)-2-cyanoacetate (4l)

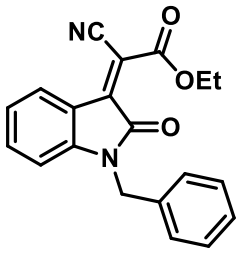

86% yield; brown crystal; m.p. 220°C; **^{1}H NMR** (500 MHz, $CDCl_3$) δ 8.33 (d, *J* = 8.0 Hz, 1H), 7.40 – 7.32 (m, 6H), 7.04 (t, *J* = 7.8 Hz, 1H), 6.75 (d, *J* = 7.7 Hz, 1H), 4.96 (s, 2H), 4.49 (m, 2H), 1.47 (t, 3H). **^{13}C NMR** (126 MHz, $CDCl_3$) δ 170.48, 164.45, 144.60, 140.90, 136.33,

129.93, 128.97, 128.42, 128.07, 127.49, 121.42, 115.82, 104.28, 60.23, 47.07, 13.64. **HRMS** (ESI) m/z: $[M + H]^+$ calculated for $C_{20}H_{17}N_2O_3$: 333.1239; found: 333.1238.

2-(5-Nitro-2-oxoindolin-3-ylidene) malononitrile(4m)

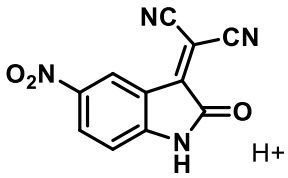

85% yield; black crystal; m.p. 178°C; **^{1}H NMR** (500 MHz, DMSO-d_6) δ 11.88 (s, 1H), 8.68 (s, 1H), 8.43 (m, 1H), 7.13 (d, *J* = 8.8 Hz, 1H). **^{13}C NMR** (126 MHz, DMSO-d_6) δ 164.44, 151.62, 149.70, 142.82, 133.12, 121.11, 119.20, 112.36, 111.35, 83.88. **HRMS** (ESI) m/z: $[M+H]^+$ calculated for $C_{11}H_5N_4O_3$: 241.0356; found: 241.0359.

2-(5-Methoxy-2-oxoindolin-3-ylidene) malononitrile(4n)

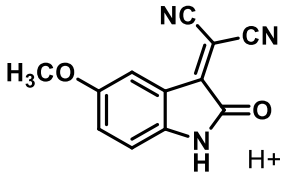

84% yield; purple crystal; m.p. 221°C; **^{1}H NMR** (500 MHz, DMSO-d_6) δ 11.00 (s, 1H), 7.38 (d, *J* = 7.6 Hz, 1H), 7.21 (d, *J* = 8.7 Hz, 1H), 6.87 (d, *J* = 8.6 Hz, 1H), 3.76 (s, 3H). **^{13}C NMR** (126 MHz, DMSO-d_6) δ 164.23, 150.94, 145.15, 139.10, 132.33, 126.24, 118.98, 113.54, 111.88, 80.78, 56.33. **HRMS** (ESI) m/z: $[M + H]^+$ calculated for $C_{12}H_8N3O_2$: 226.0611; found: 226.0608.

2-(7-Chloro-2-oxoindolin-3-ylidene)malononitrile(4o)

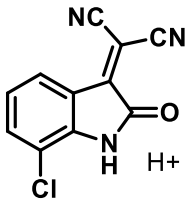

81% yield; white crystal; m.p. 229°C; **^{1}H NMR** (500 MHz, DMSO-d_6) δ 11.38 (s, 1H), 7.76 (d, *J* = 7.1 Hz, 1H), 7.63 (m, 1H), 6.97 (d, *J* = 7.5 Hz, 1H). **^{13}C NMR** (126 MHz, DMSO-d_6) δ 163.93, 150.08, 145.63, 137.38, 126.94, 125.20, 120.42, 113.74, 111.62, 82.76. **HRMS** (ESI) m/z: $[M + H]^+$ calculated for $C_{11}H_5ClN_3O$: 230.0116; found: 230.0114.

5, 5-Dimethyl-2-(2-oxoindolin-3-ylidene) cyclohexane-1, 3-dione (5a)

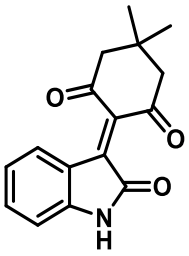

84% yield; light orange crystal; m.p. 265°C; **^{1}H NMR** (500 MHz, DMSO-d_6) δ 11.02 (d, *J* = 7.6 Hz, 1H), 7.55 (m, 1H), 7.07 (d, *J* = 7.7 Hz, 1H), 6.91 (d, *J* = 7.9 Hz, 1H), 6.87 – 6.67 (m, 1H), 2.50 – 1.77 (m, 4H), 1.10 – 0.89 (m, 6H). **^{13}C NMR** (126 MHz, DMSO-d_6) δ 194.61, 168.70, 151.24, 144.76, 138.85, 128.12, 125.16, 123.24, 118.32, 112.67, 50.63, 31.57, 26.44. **HRMS** (ESI) m/z: $[M + H]^+$ calculated for $C_{16}H_{16}NO_3$: 270.1130; found: 270.1127.

2-(5-Bromo-2-oxoindolin-3-ylidene)-5, 5-dimethylcyclohexane-1, 3-dione (5b)

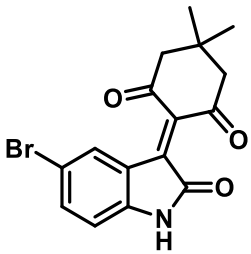

84% yield; greyish yellow crystal; m.p. 271°C; **^{1}H NMR** (500 MHz, DMSO-d_6) δ 10.33 (s, 1H), 7.35 (m, 1H), 7.16 (d, *J* = 8.0 Hz, 1H), 6.75 (d, *J* = 8.2 Hz, 1H), 2.33 – 2.01 (m, 4H), 0.98 (d, *J* = 7.1 Hz, 6H). **^{13}C NMR** (126 MHz, DMSO-d_6) δ 183.66, 176.47, 150.03, 142.52, 140.50, 132.21, 127.38, 126.29, 120.07, 114.75, 113.16, 111.92, 110.48, 78.19, 32.25, 28.42, 27.96. **HRMS** (ESI) m/z: $[M + H]^+$ calculated for $C_{16}H_{15}BrNO_3$: 348.0235; found: 348.0234.

2-(5-Chloro-2-oxoindolin-3-ylidene)-5,5-dimethylcyclohexane-1,3-dione (5c)

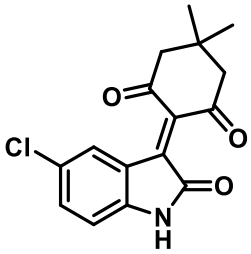

83% yield; orange crystal; m.p. 268°C; **^{1}H NMR** (500 MHz, DMSO-d_6) δ 11.17 (s, 1H), 7.00 (m, *J* = 8.1 Hz, 1H), 6.86 (d, *J* = 7.1 Hz, 1H), 6.59 (d, *J* = 8.1 Hz, 1H), 2.15 – 2.04 (m, 2H), 1.95 – 1.87 (m, 2H), 0.96 (d, *J* = 6.5 Hz, 6H). **^{13}C NMR** (126 MHz, DMSO-d_6) δ 179.94, 170.27, 150.59, 141.76, 140.69, 126.78, 124.60, 122.99, 109.92, 106.59, 50.83, 32.09, 28.79. **HRMS** (ESI) m/z: $[M + H]^+$ calculated for $C_{16}H_{15}ClNO_3$: 304.0740 ; found: 304.0738

5,5-Dimethyl-2-(5-nitro-2-oxoindolin-3-ylidene)cyclohexane-1,3-dione (5d)

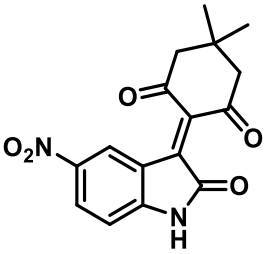

82% yield; yellow crystal; m.p. 265°C; **^{1}H NMR** (500 MHz, DMSO-d_6) δ 11.32 (s, 1H), 8.50 – 8.43 (m, 1H), 8.11 – 8.01 (m, 1H), 6.82 (t, *J* = 8.4 Hz, 1H), 2.69 – 2.57 (m, 2H), 2.15 (m, 2H), 0.99 (m, 6H). **^{13}C NMR** (126 MHz, DMSO-d_6) δ 200.15, 168.68, 156.77, 135.25, 131.87, 128.72, 117.08, 112.96, 32.19, 27.90, 27.58. **HRMS** (ESI) m/z: $[M + H]^+$ calculated for $C_{16}H_{15}N_2O_5$: 315.0980; found: 315.0978 .

5,5-Dimethyl-2-(5-methyl-2-oxoindolin-3-ylidene)cyclohexane-1,3-dione (5e)

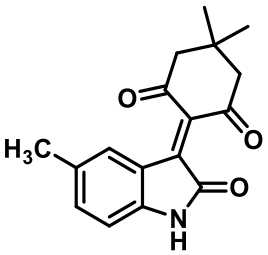

83% yield; red crystal; m.p. 258°C; **^{1}H NMR** (500 MHz, DMSO-d_6) δ 10.91 (d, *J* = 7.8 Hz, 1H), 7.40 (m, *J* = 7.9 Hz, 1H), 7.00 – 6.53 (m, 2H), 2.45 – 2.26 (m, 2H), 2.26 – 2.11 (m, 3H), 2.10 – 1.86 (m, 2H), 0.99 (m, 6H). **^{13}C NMR** (126 MHz, DMSO-d_6) δ 194.70, 182.19, 148.97, 139.35, 132.59, 128.26, 125.28, 122.45, 112.53, 101.36, 46.99, 33.66, 28.97, 27.28, 21.28. **HRMS** (ESI) m/z: $[M + H]^+$ calculated for $C_{17}H_{18}NO_3$: 284.1286; found: 284.1284 .

2-(5-Chloro-1-ethyl-2-oxoindolin-3-ylidene)-5,5-dimethylcyclohexane-1,3-dione (5f)

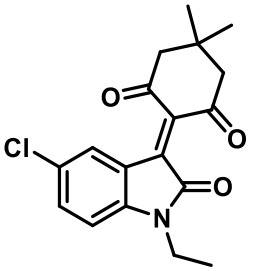

84% yield; white crystal; m.p. 279°C; **^{1}H NMR** (500 MHz, $CDCl_3$) δ 8.98 (d, *J* = 7.1 Hz, 1H), 6.85 (m, 2H), 3.90 (m, 2H), 2.31 – 2.06 (m, 4H), 1.44 (t, 3H), 1.15 (d, 3H), 1.06 (s, 3H). **^{13}C NMR** (126 MHz, $CDCl_3$) δ 195.30, 169.18, 153.70, 143.75, 133.96, 128.26, 121.13, 109.47, 101.77, 54.79, 43.26, 31.55, 27.00, 11.57. **HRMS** (ESI) m/z: $[M + H]^+$ calculated for $C_{18}H_{19}ClNO_3$: 332.1053; found: 332.1051.

2-(1-Benzyl-2-oxoindolin-3-ylidene)-5,5-dimethylcyclohexane-1,3-dione (5g)

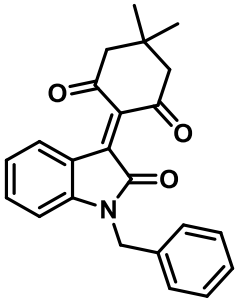

82% yield; white crystal; m.p. 276°C; **^{1}H NMR** (500 MHz, $CDCl_3$) δ 9.00 (d, *J* = 7.0 Hz, 1H), 7.64 (d, *J* = 7.7 Hz, 1H), 7.40 (t, *J* = 7.6 Hz, 1H), 7.33 – 7.27 (m, 3H), 7.11 (m, 1H), 6.90 (m, 1H), 6.66 (d, *J* = 7.8 Hz, 1H), 5.12 (m, 2H), 2.36 (m, 2H), 2.25 – 2.07 (m, 2H), 1.16 (s, 3H), 1.08 (d, 3H). **^{13}C NMR** (126 MHz, $CDCl_3$) δ 208.50, 194.91, 168.78, 153.26, 145.51, 144.33, 135.65, 128.71, 128.33, 127.33, 124.20, 122.67, 120.29, 110.00, 50.69, 48.12, 31.44, 26.68. **HRMS** (ESI) m/z: $[M + H]^+$ calculated for $C_{23}H_{22}NO_3$: 360.1599; found: 360.1595.

5,5'-(2-Oxoindoline-3,3-diyl)bis(pyrimidine-2,4,6(1H,3H,5H)-trione) (5h)

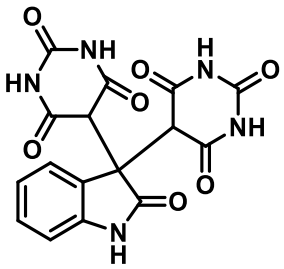

86% yield; white crystal; m.p. 185°C; **^{1}H NMR** (500 MHz, DMSO-d_6) δ 11.18 (s, 4H), 10.56 (s, 1H), 7.15 (m, 2H), 6.90 (t, *J* = 7.5 Hz, 1H), 6.69 (d, *J* = 7.7 Hz, 1H), 5.05 (s, 2H). **^{13}C NMR** (126 MHz, DMSO-d_6) δ 176.11, 168.28, 150.67, 143.65, 134.87, 129.24, 124.74, 121.91, 109.90, 53.95, 50.39. **HRMS** (ESI) m/z: $[M+H]^+$ calculated for $C_{16}H_{12}N_5O_7$: 386.0736; found: 386.0734.

5,5'-(5-Bromo-2-oxoindoline-3,3-diyl)bis(pyrimidine-2,4,6(1H,3H,5H)-trione) (5i)

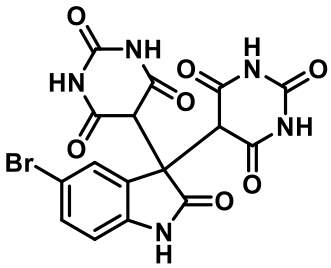

85% yield; grey crystal; m.p. 189°C; **^{1}H NMR** (500 MHz, DMSO-d_6) δ 11.14 (d, *J* = 7.9 Hz, 4H), 10.46 (s, 1H), 6.96 (d, *J* = 7.5 Hz, 2H), 6.58 (d, *J* = 8.3 Hz, 1H), 5.01 (s, 2H). **^{13}C NMR** (126 MHz, DMSO-d_6) δ 179.55, 171.23, 150.71, 141.19,

136.23, 130.40, 126.30, 123.58, 120.46, 54.07, 48.12. **HRMS** (ESI) m/z: $[M + H]^+$ calculated for $C_{16}H_{11}BrN_5O_7$; 463.9841; found: 463.9839 .

5,5'-(5-Fluoro-2-oxoindoline-3,3-diyl)bis(pyrimidine-2,4,6(1H,3H,5H)-trione) (5j)

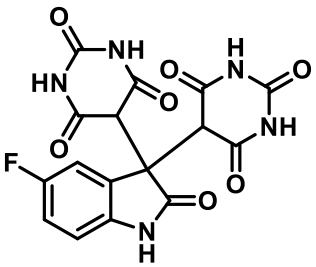

83% yield; white crystal; m.p. 181°C; **^{1}H NMR** (500 MHz, DMSO-d_6) δ 11.50 (s, 4H), 11.16 (s, 1H), 8.16 (s, 1H), 8.08 (s, 1H), 6.93 (s, 1H), 5.15 (s, 2H). **^{13}C NMR** (126 MHz, DMSO-d_6) δ 168.16, 150.60, 142.44, 129.88, 126.49, 121.27, 110.11, 52.95. **^{19}F NMR** (471 MHz, DMSO-d_6) δ -120.69, -122.28. **HRMS** (ESI) m/z: $[M + H]^+$ calculated for $C_{16}H_{11}FN_5O_7$: 404.0642; found: 404.0642 .

5,5'-(5-Methyl-2-oxoindoline-3,3-diyl)bis(pyrimidine-2,4,6(1H,3H,5H)-trione) (5k)

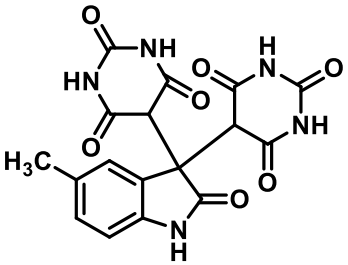

84% yield; white crystal; m.p. 192°C; **^{1}H NMR** (500 MHz, DMSO-d_6) δ 11.32 – 11.09 (m, 4H), 10.75 (s, 1H), 7.35 (d, *J* = 7.7 Hz, 1H), 7.27 (s, 1H), 6.68 (d, *J* = 8.1 Hz, 1H), 5.05 (s, 2H), 1.06 (s, 3H). **^{13}C NMR** (126 MHz, DMSO-d_6) δ 184.56, 176.00, 152.03, 139.76, 136.19, 131.28, 127.83, 125.84, 115.54, 56.50, 51.38, 19.03. **HRMS** (ESI) m/z: $[M + H]^+$ calculated for $C_{17}H_{14}N_5O_7$: 400.0893; found: 400.0891.

5,5'-(5-Chloro-1-ethyl-2-oxoindoline-3,3-diyl)bis(pyrimidine-2,4,6(1H,3H,5H)-trione) (5l)

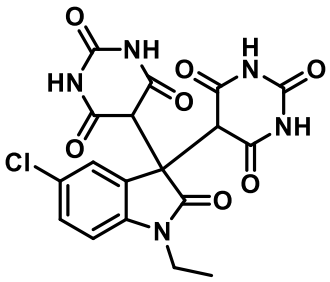

85% yield; grey crystal; m.p. 196°C; **^{1}H NMR** (500 MHz, DMSO-d_6) δ 11.21 (s, 4H), 7.33 (d, *J* = 7.9 Hz, 1H), 7.22 (s, 1H), 7.02 (d, *J* = 7.6 Hz, 1H), 5.00 (s, 2H), 3.60 (s, 2H), 1.07 (d, 3H). **^{13}C NMR** (126 MHz, DMSO-d_6) δ 174.00, 168.27, 150.57, 143.48, 126.22, 110.11, 56.50, 52.53, 34.78. **HRMS** (ESI) m/z: $[M + H]^+$ calculated for $C_{18}H_{15}ClN_5O_7$: 448.0660; found: 448.0657.

5,5'-(1-Benzyl-2-oxoindoline-3,3-diyl)bis(pyrimidine-2,4,6(1H,3H,5H)-trione) (5m)

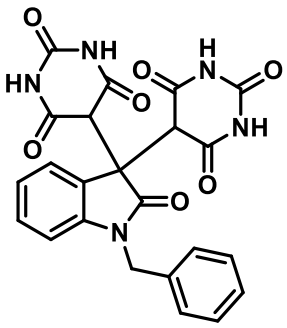

84% yield; white crystal; m.p. 198°C; **^{1}H NMR** (500 MHz, DMSO-d_6) δ 11.21 (s, 4H), 7.32 (s, 5H), 7.21 (s, 1H), 7.16 (s, 1H), 6.98 (d, *J* = 7.9 Hz, 1H), 6.61 (d, *J* = 7.8 Hz, 1H), 5.23 (s, 2H), 4.77 (s, 2H). **^{13}C NMR** (126 MHz, DMSO-d_6) δ 168.25, 150.57, 136.25, 129.32, 127.81, 124.55, 122.84, 109.65, 56.48, 53.33, 44.28. **HRMS** (ESI) m/z: $[M + H]^+$ calculated for $C_{23}H_{18}N_5O_7$: 476.1206; found: 476.1203.

Isatin (Intermediate- VII)

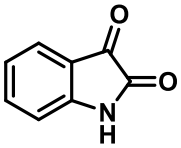

94% yield; orange crystal; m.p. 191°C; **^{1}H NMR** (500 MHz, DMSO-d_6) δ 11.22 (s, 1H), 7.89 (d, *J* = 7.7 Hz, 1H), 7.58 (t, *J* = 7.8 Hz, 1H), 7.14 (t, *J* = 7.7 Hz, 1H), 6.94 (d, *J* = 7.9 Hz, 1H). **^{13}C NMR** (126 MHz, DMSO-d_6) δ 179.71, 160.26, 148.01, 138.29, 129.84, 128.45, 114.63, 112.11.

3.8 Spectral data of few compounds

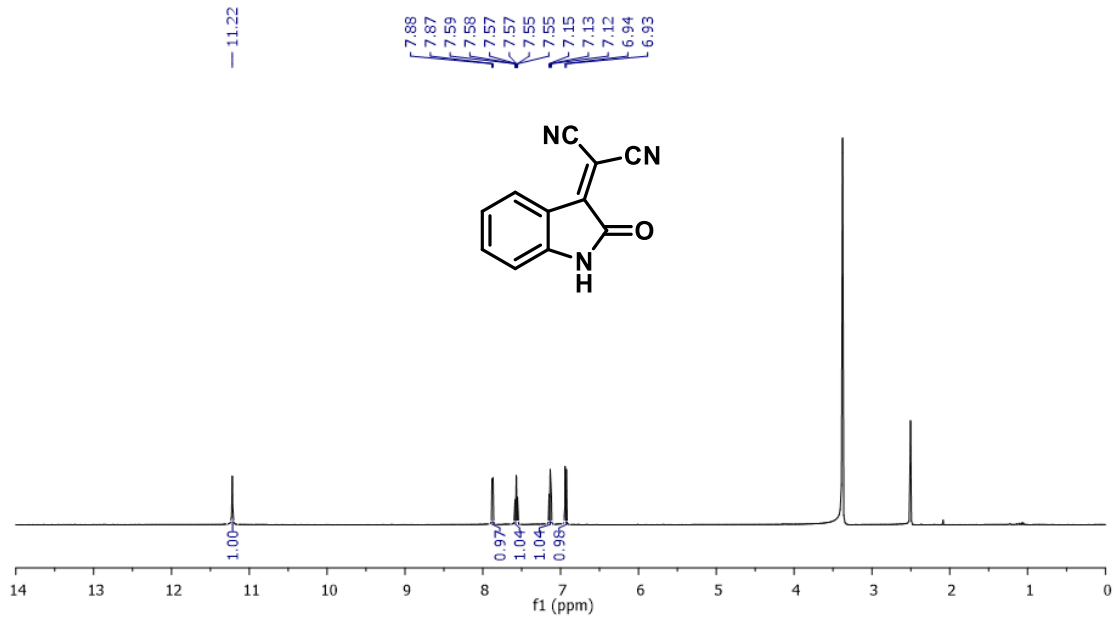

Figure 3.4 ^{1}H NMR spectrum of **4a** (500 MHz, DMSO-d_6)

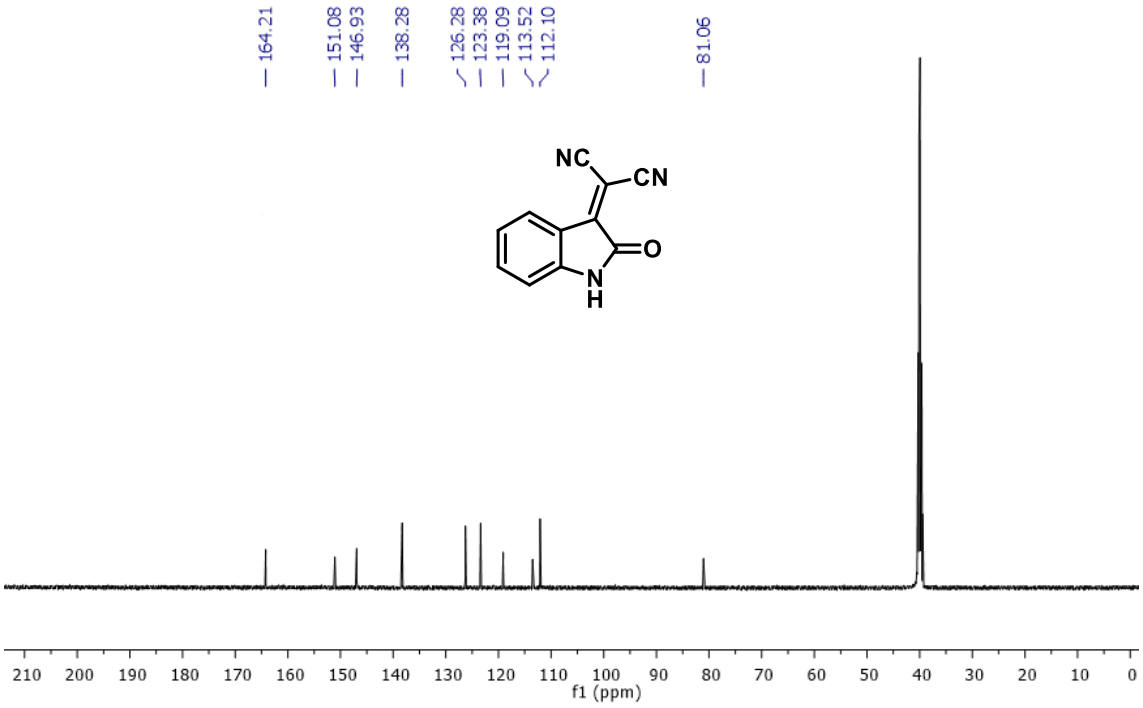

Figure 3.5 ^{13}C NMR spectrum of **4a** (126 MHz, DMSO-d_6)

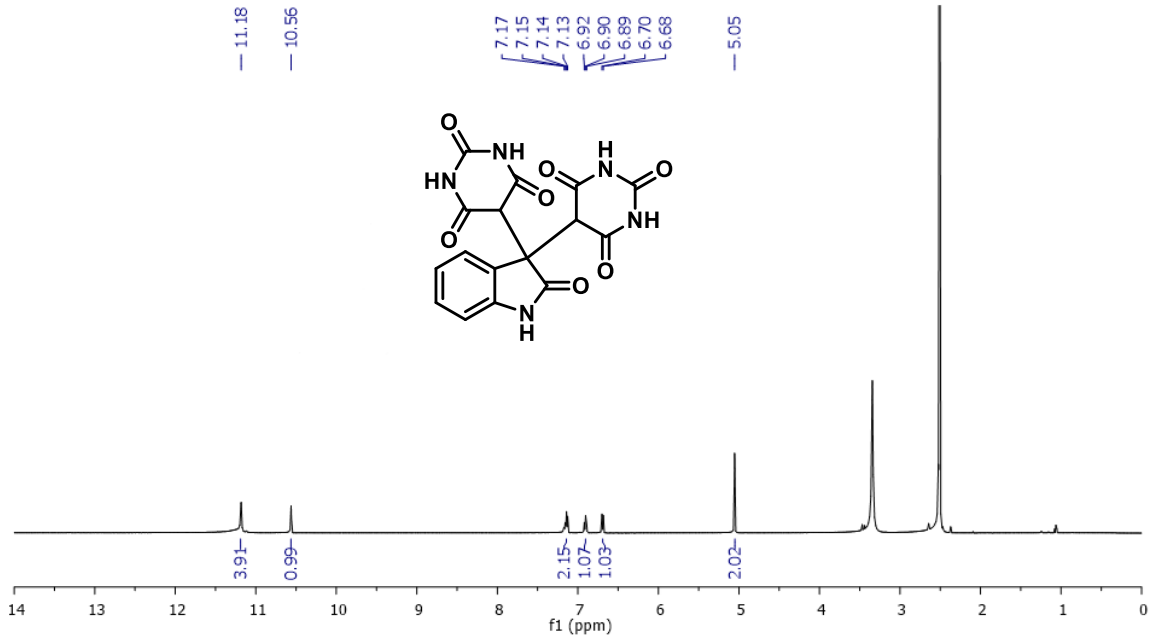

Figure 3.6 ^{1}H-NMR spectrum of **5h** (500 MHz, DMSO-d_6)

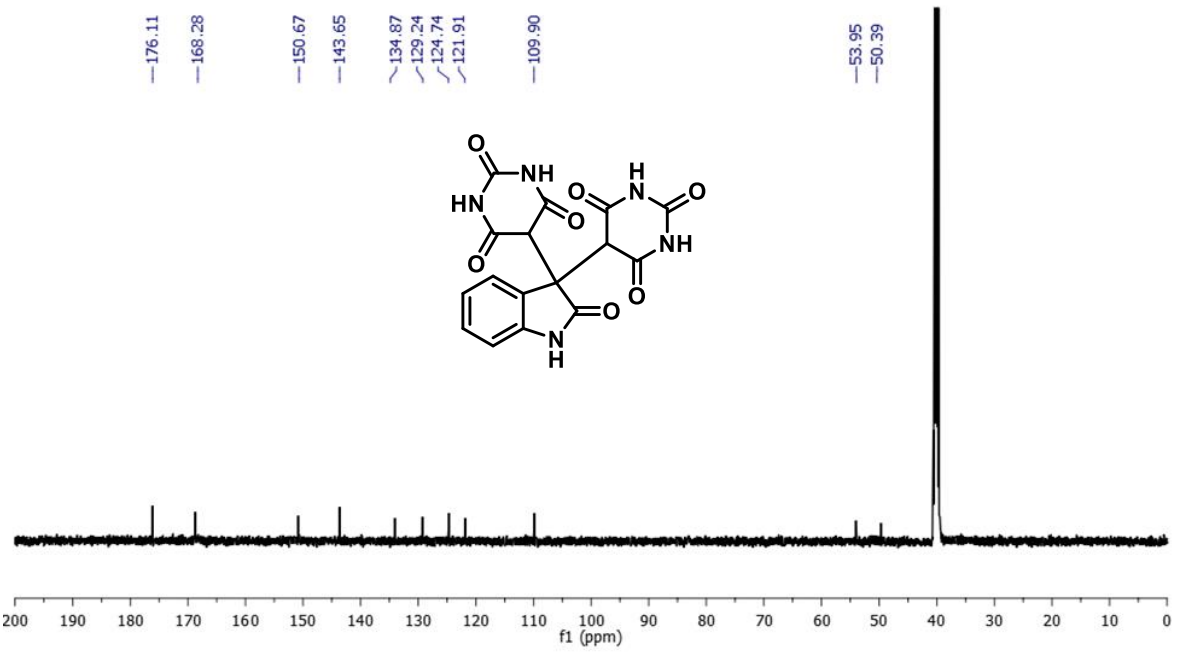

Figure 3.7 ^{13}C-NMR spectrum of **5h** (126 MHz, DMSO-d_6)

3.9 HRMS Data

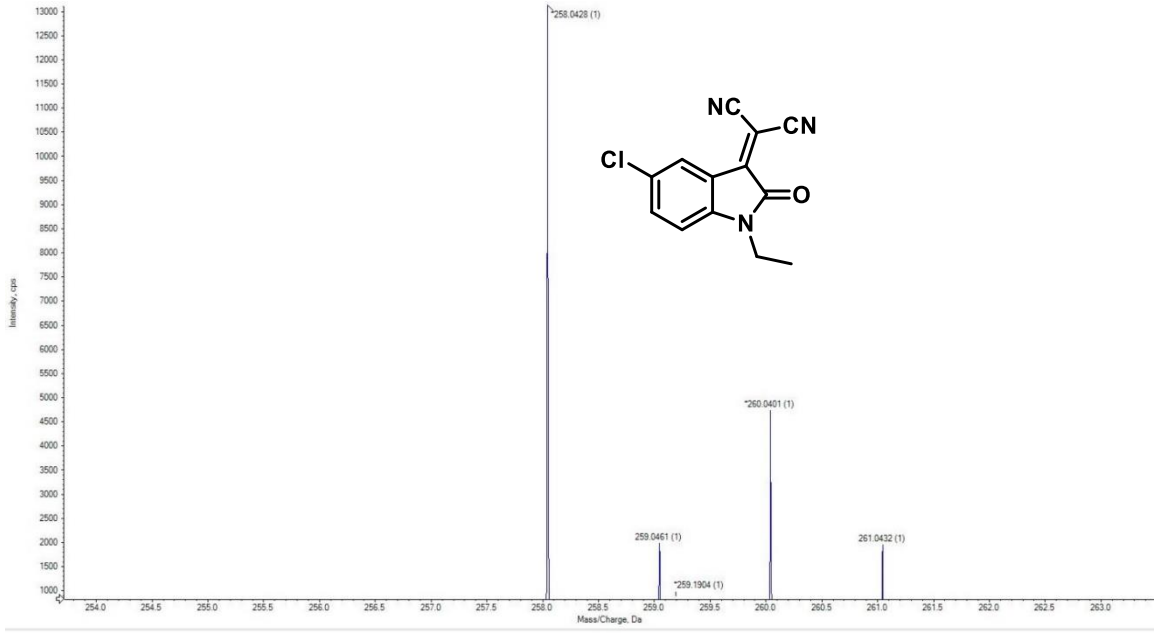

Figure 3.8 HRMS of compound **4e**

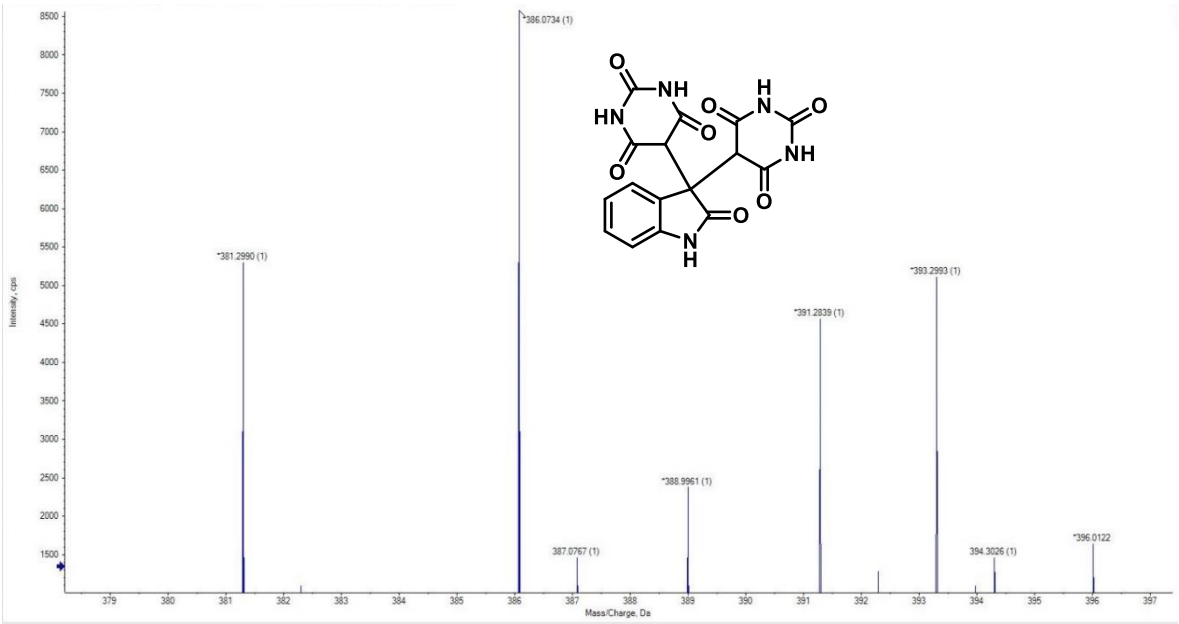

Figure 3.9 HRMS of compound **5h**

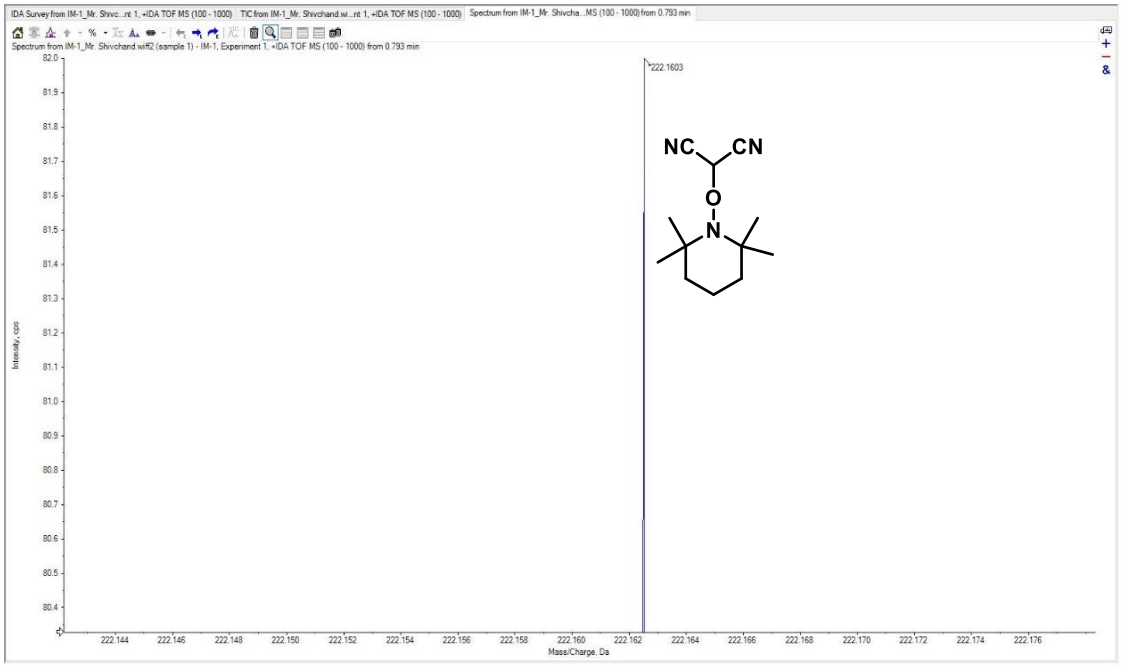

Figure 3.10 HRMS of adduct **6a**

3.10 References

[1] H. Wang, X. Gao, Z. Lv, T. Abdelilah, A. Lei, Recent advances in oxidative R1-H/R2-H cross-coupling with hydrogen evolution via photo-/electrochemistry: focus review, Chemical reviews, 119 (2019) 6769-6787.
[2] K. Morimoto, T. Dohi, Y. Kita, Metal-free oxidative cross-coupling reaction of aromatic compounds containing heteroatoms, Synlett, 28 (2017) 1680-1694.
[3] J.Y. Mak, R.H. Pouwer, C.M. Williams, Natural Products with Anti-Bredt and Bridgehead Double Bonds, Angewandte Chemie International Edition, 53 (2014) 13664-13688.
[4] J. Mol, Catalytic metathesis of unsaturated fatty acid esters and oils, Topics in Catalysis, 27 (2004) 97-104.
[5] S. Sadrameli, Thermal/catalytic cracking of hydrocarbons for the production of olefins: A state-of-the-art review I: Thermal cracking review, Fuel, 140 (2015) 102-115.
[6] T.R. Bal, B. Anand, P. Yogeeswari, D. Sriram, Synthesis and evaluation of anti-HIV activity of isatin β-thiosemicarbazone derivatives, Bioorganic & medicinal chemistry letters, 15 (2005) 4451-4455.
[7] S.A. Jassim, M.A. Naji, Novel antiviral agents: a medicinal plant perspective, Journal of applied microbiology, 95 (2003) 412-427.
[8] M. Verma, S.N. Pandeya, K.N. Singh, J.P. Stables, Anticonvulsant activity of Schiff bases of isatin derivatives, Acta Pharmaceutica, 54 (2004) 49-56.
[9] R. Tripathy, A. Reiboldt, P.A. Messina, M. Iqbal, J. Singh, E.R. Bacon, T.S. Angeles, S.X. Yang, M.S. Albom, C. Robinson, Structure-guided identification of novel VEGFR-2 kinase inhibitors via solution phase parallel synthesis, Bioorganic & medicinal chemistry letters, 16 (2006) 2158-2162.
[10] J.M.G. de Oliveira Ferreira, G.A. da Silva, M.C. Coelho, C.G.L. Junior, J.A. Vale, Quick synthesis of isatin-derived knoevenagel adducts using only eco-friendly solvent, Results in Chemistry, 3 (2021) 100-135.
[11] S.K. Maury, S. Kumari, A.K. Kushwaha, A. Kamal, H.K. Singh, D. Kumar, S. Singh, Grinding induced catalyst free, multicomponent synthesis of Indoloindole pyrimidine, Tetrahedron Letters, 61 (2020) 152383.
[12] S.K. Maury, D. Kumar, A. Kamal, H.K. Singh, S. Kumari, S. Singh, A facile and efficient multicomponent ultrasound-assisted “on water” synthesis of benzodiazepine ring, Molecular diversity, 25 (2021) 131-142.
[13] X. Jiang, Y. Sun, J. Yao, Y. Cao, M. Kai, N. He, X. Zhang, Y. Wang, R. Wang, Core scaffold-inspired concise synthesis of chiral spirooxindole-pyranopyrimidines with broad-spectrum anticancer potency, Advanced Synthesis & Catalysis, 354 (2012) 917-925.
[14] S. Pogosyan, M. Pogosyan, L. Aleksanyan, A. Safaryan, A. Arakelyan, Synthesis and Biological Activity of Substituted Spiro [chromene-4, 3′-indoles] and Spiro [indole-3, 4′-quinolines], Russian Journal of Organic Chemistry, 54 (2018) 1860–1863.
[15] S.A.S. Ghozlan, M.A. Ramadan, A.M. Abdelmoniem, I.A. Abdelhamid, synthesis and antimicrobial evaluations of novel spiro cyclic 2-oxindole derivatives of n-(1h-pyrazol-5-yl) hexahydroquinoline derivatives, Heterocycles, 92 (2016) 1075-1084.

[16] S.A. Ghozlan, M.F. Mohamed, A.G. Ahmed, S.A. Shouman, Y.M. Attia, I.A. Abdelhamid, Cytotoxic and Antimicrobial Evaluations of Novel Apoptotic and Anti-Angiogenic Spiro Cyclic 2-Oxindole Derivatives of 2-Amino-tetrahydroquinolin-5-one, Archiv der Pharmazie, 348 (2015) 113-124.
[17] J.H. Choi, C.M. Park, Three-Component Synthesis of Quinolines Based on Radical Cascade Visible-Light Photoredox Catalysis, Advanced Synthesis & Catalysis, 360 (2018) 3553-3562.
[18] L. Revathi, L. Ravindar, W.Y. Fang, K. Rakesh, H.L. Qin, Visible light-induced C− H bond functionalization: a critical review, Advanced Synthesis & Catalysis, 360 (2018) 4652-4698.
[19] M. Zhu, W. Fu, W. Guo, Y. Tian, Z. Wang, B. Ji, Visible-light-induced radical trifluoromethylthiolation of N-(o-cyanobiaryl) acrylamides, Organic & biomolecular chemistry, 17 (2019) 3374-3380.
[20] H. Yang, C. Tian, D. Qiu, H. Tian, G. An, G. Li, Organic photoredox catalytic decarboxylative cross-coupling of gem-difluoroalkenes with unactivated carboxylic acids, Organic Chemistry Frontiers, 6 (2019) 2365-2370.
[21] W. Fu, X. Han, M. Zhu, C. Xu, Z. Wang, B. Ji, X.-Q. Hao, M.-P. Song, Visible-light-mediated radical oxydifluoromethylation of olefinic amides for the synthesis of CF 2 H-containing heterocycles, Chemical Communications, 52 (2016) 13413-13416.
[22] I. Ghosh, T. Ghosh, J.I. Bardagi, B. König, Reduction of aryl halides by consecutive visible light-induced electron transfer processes, Science, 346 (2014) 725-728.
[23] N.A. Romero, K.A. Margrey, N.E. Tay, D.A. Nicewicz, Site-selective arene CH amination via photoredox catalysis, Science, 349 (2015) 1326-1330.
[24] A. Kamal, H.K. Singh, D. Kumar, S.K. Maury, S. Kumari, V. Srivastava, S. Singh, Visible Light-Induced Cu-Catalyzed Synthesis of Schiff's Base of 2-Amino Benzonitrile Derivatives and Acetophenones, Chemistry Select, 6 (2021) 52-58.
[25] H.K. Singh, A. Kamal, S. Kumari, S.K. Maury, A.K. Kushwaha, V. Srivastava, S. Singh, Visible-Light-Promoted Synthesis of Fusesd Imidazoheterocycle by Eosin Y under Metal-Free and Solvent-Free Conditions, Chemistry Select, 6 (2021) 13982-13991.
[26] H.K. Singh, A. Kamal, S. Kumari, D. Kumar, S.K. Maury, V. Srivastava, S. Singh, Eosin Y-Catalyzed Synthesis of 3-Aminoimidazo [1, 2-a] Pyridines via the HAT Process under Visible Light through Formation of the C–N Bond, ACS omega, 5 (2020) 29854-29863.
[27] X.-J. Yang, B. Chen, L.-Q. Zheng, L.-Z. Wu, C.-H. Tung, Highly efficient and selective photocatalytic hydrogenation of functionalized nitrobenzenes, Green Chemistry, 16 (2014) 1082-1086.
[28] D.T. Yang, Q.Y. Meng, J.J. Zhong, M. Xiang, Q. Liu, L.Z. Wu, Metal-free desulfonylation reaction through visible-light photoredox catalysis, European Journal of Organic Chemistry, 2013 (2013) 7528-7532.
[29] K. Fidaly, C. Ceballos, A. Falguières, M.S.-I. Veitia, A. Guy, C. Ferroud, Visible light photoredox organocatalysis: a fully transition metal-free direct asymmetric α-alkylation of aldehydes, Green Chemistry, 14 (2012) 1293-1297.

[30] Y.C. Teo, Y. Pan, C.H. Tan, Organic Dye-Photocatalyzed Acylnitroso Ene Reaction, ChemCatChem, 5 (2013) 235-240.
[31] Z.-Y. Tan, K.-X. Wu, L.-S. Huang, R.-S. Wu, Z.-Y. Du, D.-Z. Xu, Iron-catalyzed cross-dehydrogenative coupling of indolin-2-ones with active methylenes for direct carbon–carbon double bond formation, Green Chemistry, 22 (2020) 332-335.
[32] L.S. Huang, Y.H. Lai, C. Yang, D.Z. Xu, Iron-catalyzed one-pot oxidation/Knoevenagel condensation reaction using air as an oxidant, Applied Organometallic Chemistry, 33 (2019) e4910.
[33] F. Yue, J. Dong, Y. Liu, Q. Wang, Visible-light-mediated alkenylation of alkyl boronic acids without an external Lewis base as an activator, Organic Letters, 23 (2021) 2477-2481.
[34] F. Yue, J. Dong, Y. Liu, Q. Wang, Visible-Light-Mediated C–I Difluoroallylation with an α-Aminoalkyl Radical as a Mediator, Organic Letters, 23 (2021) 7306-7310.
[35] Y. Zhao, C. Zhang, K.F. Chin, O. Pytela, G. Wei, H. Liu, F. Bureš, Z. Jiang, Dicyanopyrazine-derived push–pull chromophores for highly efficient photoredox catalysis, RSC advances, 4 (2014) 30062-30067.
[36] W. Schilling, Y. Zhang, D. Riemer, S. Das, Visible-Light-Mediated Dearomatisation of Indoles and Pyrroles to Pharmaceuticals and Pesticides, Chemistry (Weinheim an der Bergstrasse, Germany), 26 (2020) 390.
[37] S. Kumari, S. Kumar Maury, H. Kumar Singh, A. Kamal, D. Kumar, S. Singh, V. Srivastava, Visible Light Mediated, Photocatalyst-Free Condensation of Barbituric Acid with Carbonyl Compounds, ChemistrySelect, 6 (2021) 2980-2987.